www.elsevier.com/locate/dsri

(This is a sample cover image for this issue. The actual cover is not yet available at this time.)

Linking phytoplankton community size composition with temperature, plankton food web structure and sea–air CO_2 flux

Karen Marie Hilligsøe [a], Katherine Richardson [a,b,*], Jørgen Bendtsen [c], Lise-Lotte Sørensen [d], Torkel Gissel Nielsen [e], Maren Moltke Lyngsgaard [a,b]

[a] Department of Bioscience, Aarhus University, Ole Worms Allé 1, DK-8000 Århus C, Denmark
[b] Center for Macroecology, Evolution and Climate, Faculty of Science, University of Copenhagen, Tagensvej 16, DK-2200 Copenhagen, Denmark
[c] VitusLab, Symbion Science Park, Fruebjergvej 3, Box 98, DK-2100 Copenhagen Ø, Denmark
[d] Department of Environmental Science, Aarhus University, Frederiksborgvej 399, PO Box 358, DK-4000 Roskilde, Denmark
[e] National Institute of Aquatic Resources, Section for Ocean Ecology and Climate, Technical, University of Denmark, Kavalergården 6, DK- 2920 Charlottenlund, Denmark

ABSTRACT

Data collected at open water stations (depth > 400 m) in all major ocean basins in 2006–2008 are used to examine the relationship between the size structure of the phytoplankton community (determined by size fractionated chlorophyll filtration), temperature and inorganic nutrient availability. A significant relationship ($p < 0.0005$) was found between community size structure and temperature, with the importance of large cells in the community decreasing with increase in temperature. Although weaker than the temperature relationship, significant relationships were also noted between community cell size and DIN (nitrate, nitrite and ammonium: $p = 0.034$) and phosphate ($p = 0.031$) concentrations. When the data were divided into two groups of equal size, representing the samples with the highest and lowest DIN/phosphate concentrations, respectively, no difference could be identified between the slopes of the lines representing the relationship between size structure and temperature. There was, however, a difference in the intercepts between the two groups. If the relationship between size and temperature was only a response to nutrient availability, we would expect that the response would be the strongest in the groups with the lowest nutrient concentrations. These results suggest that, in addition to a nutrient effect, temperature may also directly influence the size structure of phytoplankton communities. The size structure of the phytoplankton community in this study correlated to the magnitude of primary production, export production (determined after Laws et al., 2000) and integrated water column chlorophyll. Significant relationships were also found between mesozooplankton production (determined using the proxy of calanoid+cyclopoid nauplii abundance as a percentage of the total number of these copepods) and both temperature and phytoplankton size, with production being the lowest in the warmest waters where phytoplankton were the smallest. In the North Atlantic, export production and community size structure appear to be related to ocean uptake of CO_2 from the atmosphere. The reported results suggest that ocean warming may directly alter plankton community structure. This, in turn, may alter the structure of marine food webs and impact the performance of the open ocean as a natural carbon sink.

© 2011 Elsevier Ltd. All rights reserved.

1. Introduction

The oceans are a major reservoir of dissolved inorganic carbon and it is estimated that the oceans have taken up on the order of a third to one half of the CO_2 released to the atmosphere via anthropogenic activities since the industrial revolution (Sabine et al., 2004; Khatiwala et al., 2009). The function of this carbon sink is, thus, extremely important in the global carbon cycle. As there is a potential risk that the strength of the global ocean carbon sink will diminish in a warmer climate (Sarmiento et al., 1998), it is important to understand the processes contributing to this sink and, especially, to understand how change in oceanic conditions may influence these processes.

Much emphasis has been given to the physical and chemical processes relating to the sea–air flux of CO_2 and detailed mappings of the seasonal distribution of surface-ocean and atmospheric pCO_2 have been carried out. These measurements allow estimates of

---

seasonal patterns in sea–air CO_2 flux based on comprehensive data sets of the surface pCO_2 distribution and parameterizations of the sea–air CO_2 gas exchange (Takahashi et al., 2002).

It is generally recognized that biological processes also potentially influence the sea–air CO_2 flux. A global estimate of this biological mediated draw-down of surface pCO_2 has been made by removing the seasonal pCO_2 change due to changes in surface temperatures (SST). This signal has been shown to be large, in particular north of 40°N, where seasonal pCO_2 changes, which cannot be explained by seasonal changes in surface temperature, exceed more than 140 μatm (Takahashi et al., 2002). A number of more recent studies carried out in the North Atlantic have also indicated that biological processes may be particularly important in sea–air CO_2 flux here (e.g. Körtzinger et al., 2008; Bennington et al., 2009; Takahashi et al., 2009).

While it is generically recognized that biological processes are important for sea–air CO_2 flux, few attempts have, to date, been made to decompose this biological signal into its various contributing components. Thus, it is still unclear how the individual component processes leading to the biological signal contribute to sea–air CO_2 flux. The most obvious of biological processes potentially impacting surface pCO_2 in the open ocean is photosynthesis by phytoplankton. During this "primary production" phytoplankton synthesize dissolved inorganic carbon (TCO_2) to organic material. The resulting reduction in surface pCO_2 then tends to increase the CO_2 flux from the atmosphere to the ocean. Carbon is subsequently transported into the deep ocean through sinking particulate organic matter (phytoplankton cells, higher trophic organisms and detritus) and through mixing of dissolved organic carbon and this "biological pump" tends to increase the ocean-atmosphere pCO_2 difference on longer time scales (months–years) and, thereby, the sea–air CO_2 flux.

Often, the POC sinking out of the surface layer is dominated by phytoplankton cells. The sinking rate of phytoplankton cells is related to their size (see Kiørboe, 1993 for review). As the size of phytoplankton ranges from < 1 μm to around 1 mm, there can be considerable differences in the rate of carbon transfer from surface ocean waters to depth depending on the composition of the phytoplankton community. The size structure of any given phytoplankton community is normally assumed to be controlled by nutrient availability (see Kiørboe, 1993 for review). However, a number of studies suggest that temperature may also be a controlling factor for community size structure. The potential role that temperature may have is, however, difficult to discern as temperature and inorganic nutrient availability tend to co-vary on the global scale.

Finkel et al. (2007) identify climate (as expressed through temperature) as being an important controlling factor for macroevolutionary changes in phytoplankton community size structure (and, thereby, ocean carbon cycling) during the Cenozoic period. They interpret this temperature influence on phytoplankton size as being through its influence on ocean stratification and the resulting availability of nutrients in the surface layer.

Agawin et al. (2000) demonstrated that the relative dominance of picoplankton is the greatest in warm oligotrophic waters. They recognized a covariance with temperature and nutrients in their meta-analysis but did not have sufficient data to discern the potential importance of the two factors. With the help of mesocosm data, however, they concluded that the advantage that small sized phytoplankton have under oligotrophic conditions is a primary contributor to the dominance of picoplankton in warm oligotrophic waters. Morán et al. (2010), on the other hand, concluded that temperature alone could explain 73% of the variance noted in the global distribution of picoplankton.

In an intriguing study based on a short time series (5 years), carried out in Arctic waters where nutrient availability is not believed to be limiting, Li et al. (2009) demonstrated a strong relationship between phytoplankton community size structure (decrease in nanoplankton; increase in picoplankton) and increase in temperature/decrease in salinity. Over the same period, an increase in bacterioplankton abundance was recorded. In that study, it is not possible to separate the potential temperature effect from a possible salinity effect.

Taken together, the recent literature tends to suggest that the possibility of a direct temperature influence on phytoplankton community size structure cannot be eliminated. If there is such an effect, then change in climate conditions, including a warming of the oceans, could potentially create a feedback on the climate system via changes in phytoplankton communities and, thereby, biologically mediated ocean carbon cycling.

In the present study, the potential role of temperature in influencing phytoplankton community size structure is addressed using a data set acquired on a cruise circumnavigating the globe in 2006–2007. These data are supplemented with data collected in the North Atlantic on an additional cruise conducted in 2008. The potential biogeochemical impacts of changes in phytoplankton community size structure are addressed by examining sea–air flux of CO_2 in relation to both the magnitude of primary production and "export" production, i.e. the fraction of primary production leaving the surface layer, via the model described by Laws et al. (2000), and the phytoplankton community size structure. Potential impacts of changes in phytoplankton community size structure on the structure of the zooplankton community are also addressed.

We confine our study to the open ocean (defined here as stations with water depths ≥ 400 m) as the open ocean is believed to be most important in terms of the carbon export into the deep ocean: Dunne et al. (2007) estimated that the open ocean (depths > 200 m) accounts for approximately 80% of the global export. In addition, coastal stations may be influenced by other factors than the open ocean. Thus, considering the open ocean and coastal stations together may mask global patterns in the relationship between biological activity and ocean carbon uptake.

2. Material and methods

2.1. Cruise information

Samples used for this study were collected during the circumnavigating Galathea 3 expedition on HDMS Vædderen carried out from 11 August 2006 to 25 April 2007 and on a cruise with R/V DANA from 5 to 13 August 2008 in the Northern North Atlantic. Thus, the data set includes stations sampled along transects across the northern part of the North Atlantic sub-polar gyre both in August–September 2006 and August 2008. These transects also covered waters from the East Greenland Current and Irminger Sea towards the North Atlantic Current. Four samples were also taken in the southern part of the West Greenland Current system. Samples from the Gulf Stream and the southern part of the North Atlantic sub-polar gyre were collected in April 2007. A detailed study of the hydrography in the Sargossa Sea resulted in 19 samples from this area and 1 sample from the Caribbean Sea in March–April 2007. Samples (11) from the Eastern Atlantic were taken along a transect from the Azores towards the Angola and Benguela Current systems in September–October 2006. A transect along the south Indian Ocean Current (6 samples) and the southern Leeuwin Current (4 samples) was sampled in October–December 2006. Samples from the East Australian Current (3 samples) and Solomon Sea (5 samples) were collected in December 2006 and 13 samples were subsequently measured in the Southern Ocean in January–February 2007. Samples from the Peru/Chile Current and eastern equatorial Pacific were collected in February–March 2007. In summary, samples were collected from oligotrophic subtropical gyres, equatorial and coastal

Table 1

Stations sampled. 0 indicates no data collected. 1 indicates data collected and used in the analyses.

Index	Latitude (dec. deg.)	Longitude (dec. deg.)	Date (yyyy/mm/dd)	Primary production and pCO$_2$-flux data	Phytoplankton size and nutrient data	Zooplankton and phytoplankton size data	Region
1	61.391	−3.443	2006/08/16	0	1	0	Northern North Atlantic
2	62.038	−9.996	2006/08/18	1	1	0	Northern North Atlantic
3	62.165	−16.573	2006/08/18	1	1	0	Northern North Atlantic
4	62.516	−33.309	2006/08/20	1	1	0	Northern North Atlantic
5	60.230	−48.467	2006/08/26	0	1	0	Northern North Atlantic
6	65.835	−56.565	2006/08/31	0	1	0	Northern North Atlantic
7	66.905	−53.289	2006/09/04	0	1	0	Northern North Atlantic
8	62.110	−50.977	2006/09/12	0	1	0	Northern North Atlantic
9	53.783	−38.384	2006/09/14	1	1	0	Northern North Atlantic
10	40.692	−28.814	2006/09/16	1	1	1	Northern North Atlantic
11	38.004	−27.000	2006/09/17	1	1	1	Eastern Atlantic
12	33.768	−25.415	2006/09/22	1	1	1	Eastern Atlantic
13	23.079	−24.052	2006/09/24	1	1	1	Eastern Atlantic
14	12.206	−21.023	2006/09/26	1	1	1	Eastern Atlantic
15	1.627	−10.524	2006/09/29	1	1	1	Eastern Atlantic
16	4.741	−0.331	2006/10/02	0	1	1	Eastern Atlantic
17	−4.932	4.483	2006/10/08	0	1	0	Eastern Atlantic
18	−7.430	5.552	2006/10/09	1	1	1	Eastern Atlantic
19	−12.512	7.807	2006/10/10	0	1	0	Eastern Atlantic
20	−24.149	13.299	2006/10/12	1	0	0	Eastern Atlantic
21	−27.885	14.656	2006/10/13	1	1	1	Eastern Atlantic
22	−38.486	31.715	2006/10/21	0	1	1	Indian Ocean sector
23	−39.564	42.746	2006/10/23	0	1	1	Indian Ocean sector
24	−37.259	72.507	2006/10/27	0	1	1	Indian Ocean sector
25	−31.406	91.178	2006/10/30	0	1	1	Indian Ocean sector
26	−29.582	95.249	2006/10/31	0	1	1	Indian Ocean sector
27	−24.468	105.236	2006/11/02	0	1	1	Indian Ocean sector
28	−34.380	114.411	2006/11/24	0	1	1	Indian Ocean sector
29	−33.497	128.393	2006/11/29	0	1	1	Indian Ocean sector
30	−35.174	132.617	2006/12/03	0	1	1	Indian Ocean sector
31	−37.295	137.673	2006/12/04	0	1	1	Indian Ocean sector
32	−42.572	149.667	2006/12/05	0	1	0	Indian Ocean sector
33	−37.921	151.140	2006/12/09	0	1	0	Eastern South Pacific
34	−31.512	153.412	2006/12/14	0	1	1	Eastern South Pacific
35	−14.213	156.859	2006/12/18	0	1	1	Eastern South Pacific
36	−10.702	157.482	2006/12/20	0	1	0	Eastern South Pacific
37	−10.179	157.594	2006/12/21	0	1	0	Eastern South Pacific
38	−9.894	157.474	2006/12/23	0	0	1	Eastern South Pacific
39	−7.824	156.069	2006/12/27	0	1	1	Eastern South Pacific
40	−29.046	164.427	2007/01/04	0	1	1	Eastern South Pacific
41	−36.003	170.860	2007/01/05	0	1	1	Eastern South Pacific
42	−49.695	178.877	2007/01/12	1	1	1	Southern Ocean
43	−55.636	−167.539	2007/01/14	1	1	0	Southern Ocean
44	−61.827	−150.931	2007/01/16	1	1	1	Southern Ocean

Table 1 (continued)

Index	Latitude (dec. deg.)	Longitude (dec. deg.)	Date (yyyy/mm/dd)	Primary production and pCO$_2$-flux data	Phytoplankton size and nutrient data	Zooplankton and phytoplankton size data	Region
45	−64.583	−132.385	2007/01/18	1	1	0	Southern Ocean
46	−66.590	−108.931	2007/01/20	1	1	1	Southern Ocean
47	−67.278	−83.020	2007/01/22	1	1	0	Southern Ocean
48	−63.902	−61.633	2007/01/27	1	1	0	Southern Ocean
49	−62.965	−58.050	2007/01/29	1	1	0	Southern Ocean
50	−62.319	−57.748	2007/01/30	1	1	1	Southern Ocean
51	−58.802	−60.900	2007/01/30	1	1	0	Southern Ocean
52	−57.928	−61.870	2007/01/31	1	1	0	Southern Ocean
53	−38.576	−74.452	2007/02/06	1	0	0	Eastern Pacific
54	−38.105	−74.125	2007/02/07	1	1	0	Eastern Pacific
55	−29.286	−71.883	2007/02/12	1	1	0	Eastern Pacific
56	−26.304	−71.262	2007/02/12	1	1	0	Eastern Pacific
57	−20.057	−70.755	2007/02/17	1	1	0	Eastern Pacific
58	−17.086	−72.419	2007/02/18	1	1	0	Eastern Pacific
59	−14.237	−76.602	2007/02/20	1	0	0	Eastern Pacific
60	−13.872	−76.804	2007/02/22	0	1	0	Eastern Pacific
61	−14.276	−76.793	2007/02/23	1	0	1	Eastern Pacific
62	−14.163	−77.429	2007/02/24	1	1	1	Eastern Pacific
63	−5.254	−81.578	2007/03/01	1	1	0	Eastern Pacific
64	0.009	−85.450	2007/03/03	0	1	1	Eastern Pacific
65	5.330	−84.115	2007/03/09	1	1	1	Eastern Pacific
66	6.665	−80.997	2007/03/10	1	1	1	Eastern Pacific
67	10.700	−79.026	2007/03/12	1	1	0	Western Atlantic
68	17.025	−67.794	2007/03/14	1	1	0	Western Atlantic
69	19.000	−63.999	2007/03/29	1	1	1	Western Atlantic
70	22.044	−64.005	2007/03/30	1	1	1	Western Atlantic
71	25.254	−63.998	2007/03/31	1	0	1	Western Atlantic
72	26.501	−64.001	2007/04/01	1	1	1	Western Atlantic
73	27.329	−64.000	2007/04/02	0	0	1	Western Atlantic
74	27.660	−63.997	2007/04/02	1	1	1	Western Atlantic
75	28.502	−67.004	2007/04/03	1	1	1	Western Atlantic
76	26.501	−66.998	2007/04/04	1	1	1	Western Atlantic
77	25.664	−66.996	2007/04/04	0	0	1	Western Atlantic
78	25.003	−67.002	2007/04/05	1	1	1	Western Atlantic
79	24.991	−69.997	2007/04/06	1	1	0	Western Atlantic
80	27.030	−70.090	2007/04/07	1	1	0	Western Atlantic
81	28.993	−69.997	2007/04/08	1	1	0	Western Atlantic
82	32.508	−70.027	2007/04/09	1	1	1	Western Atlantic
83	44.334	−56.176	2007/04/16	1	1	1	Northern North Atlantic
84	44.328	−48.958	2007/04/17	1	1	0	Northern North Atlantic
85	44.395	−47.444	2007/04/18	1	1	0	Northern North Atlantic
86	53.490	−23.331	2007/04/21	1	1	0	Northern North Atlantic
87	56.186	−15.234	2007/04/22	1	1	0	Northern North Atlantic
88	62.633	−40.510	2008/08/06	1	1	0	Northern North Atlantic
89	62.621	−37.892	2008/08/07	1	1	0	Northern North Atlantic
90	62.560	−35.239	2008/08/07	1	1	0	Northern North Atlantic
91	62.515	−32.680	2008/08/08	1	1	0	Northern North Atlantic
92	62.444	−30.122	2008/08/08	1	1	0	Northern North Atlantic
93	62.389	−27.524	2008/08/08	0	1	0	Northern North Atlantic
94	62.340	−24.930	2008/08/09	0	1	0	Northern North Atlantic
95	62.293	−22.336	2008/08/09	0	1	0	Northern North Atlantic
96	62.237	−19.729	2008/08/10	0	1	0	Northern North Atlantic

upwelling zones, sub-polar and polar waters and the Southern Ocean. Thus, this data set includes samples from a major part of the global ocean. Detailed station information is listed in Table 1. The methods used on both cruises were identical.

2.2. Hydrographic data and sample collection

Conductivity, temperature and depth were measured using a Seabird instruments 911 System at the stations identified.

The instruments were attached to a rosette of 12 Niskin bottles (30l), a fluorometer (SCUFA or Dr Haardt), light meters (Biospherical) and two oxygen sensors (SBE43). All instruments were calibrated and data quality controlled before use. Samples were taken from selected depths for oxygen calibration (Winkler), salinity calibration (PortaSal), chlorophyll determination, size fractionated chlorophyll determination, nutrient analysis, primary production and phytoplankton species determination.

2.3. Identification of surface waters

For the analyses, the stations in Table 1 are assigned to seven different regions. Stations north of 40° north are assigned to the Northern North Atlantic. The Eastern Atlantic region includes stations south of 40° north in the eastern part of the Atlantic, more specifically in the Cape Verde, Gambia and Guinea Abyssal Plains as well as the Angola and Cape Basins. All stations in the Indian Ocean as well as all stations south of Australia and west of 150° east are assigned to the Indian Ocean Sector. All stations in the Solomon Sea itself, as well as stations in the New Caledonia Basin and Tasman Sea east of 150° east, are assigned to the Eastern South Pacific. Stations sampled in the Pacific part of the Southern Ocean as well as the Drake Passage are assigned to the Southern Ocean. Stations in the Chile and Peru Basins are assigned to the Eastern Pacific. The Caribbean and Sargasso Sea stations are assigned to the Western Atlantic.

2.4. Chlorophyll determination and size fractionation of chlorophyll

Chlorophyll and size fractions of chlorophyll were determined in the surface water, the chlorophyll maximum and at the standard sampling depth below the chlorophyll maximum. In addition, sampling at 30 m was carried out at intensively investigated stations. On the Dana 2008 cruise, chlorophyll and size fractions of chlorophyll were only determined for the surface water and chlorophyll maximum. Seawater was tapped from Niskin bottles from the CTD rosette and filtered on GF/F (approximately 0.75 μm) and 10 μm pore size filters. For each sampling depth and filter size, triplicate filtrations of 200–500 ml seawater for the GF/F filter and 400–1000 ml seawater for the 10 μm filter were performed. The volume filtered depended on the in-situ chlorophyll concentration. The filters were stored in glass vials with 5 ml 96% ethanol and frozen at –20 °C. Prior to analysis, the samples were extracted for a minimum of 6 h and a maximum of 24 h in darkness at room temperature. The samples were measured on a TD-700 fluorometer from Turner Designs, which was calibrated against a pure chlorophyll a standard. The procedure for calculation of chlorophyll a from fluorescence is Method 445.0 by the U.S. Environmental Protection Agency as suggested by Turner Designs (http://www.epa.gov/microbes/m445_0.pdf). The fluorometer measurements made with the CTD were calibrated against the discrete measurements made in each region/water mass. Integrated water column chlorophyll was estimated from the calibrated fluorometer profiles.

The fraction of total chlorophyll a retained on a 10 μm filter was calculated as $f_{10\,\mu m} = c_{\text{chlorophyll } a\,10\,\mu m} / c_{\text{chlorophyll } a\,\text{GF/F}}$, where $c_{\text{chlorophyll } a\,\text{GF/F}}$ and $c_{\text{chlorophyll } a\,10\,\mu m}$ are the concentrations of chlorophyll a in the water sample, originating from the phytoplankton collected on the GF/F and 10 μm pore size filter, respectively. In the following, we refer to the fraction of total chlorophyll a retained on a 10 μm filter as the fraction of the phytoplankton community > 10 μm.

2.5. Determination of inorganic nutrients

At each station, seawater from the chlorophyll maximum and the standard sampling depths of 10, 30, 60, 100, 200 and 400 m was tapped from Niskin bottles from the CTD rosette and immediately frozen. For stations where the latitude was $\geq 50°$, the surface sampling depth was changed to 5 m instead of 10 m. The subsequently filtered seawater (Millipore Millex-GP Hydrophilic PES 0.22 μm) was analyzed for nitrate, nitrite, phosphate, ammonium and silicate by wet-chemistry methods according to Grasshoff (Ed.) et al. (1983) with a SANPLUS System Scalar auto-analyser at the National Environmental Research Institute (NERI), University of Aarhus, Denmark. Detection limits of 0.06, 0.1, 0.04, 0.3 and 0.2 μM are for phosphorus, nitrate, nitrite, ammonium and silicate, respectively.

2.6. Primary production determination

The primary production was measured according to a modified carbon-14 method (Steemann Nielsen, 1952). Particulate production (retained on a GF/F filter) was determined from samples taken from two depths: the surface layer and the depth of the subsurface chlorophyll peak (or at 20 m in the absence of a subsurface peak). Again, for latitudes $\geq 50°$ N and S, the surface sampling depth was changed to 5 m instead of 10 m. Primary production vs. light intensity curves were fitted to the data that were generated in incubations carried out in 50 ml polyethylene bottles for 2 h at 12 different light intensities (ranging from < 10 to > 1000 μmol m^{-2} s^{-1}) and two dark samples from each sampling depth. The dark samples were subtracted from the light incubation samples. Primary production was calculated by creating a matrix of potential production through the water column over the light period of the day using the established primary production vs. light intensity curves and the light climate at meter intervals through the water column throughout the day (estimated from the measured attenuation coefficient and "incident" light during the week of sampling, i.e. hourly averages made over a seven-day average around the date of the sampling). Using these weekly averages of incident light, the potential primary production at stations sampled on days with different light conditions could be compared. The euphotic zone was assigned as being the waters above the depth of the penetration of 0.1% surface irradiance.

No correction was made for possible isotope discrimination or photo-inhibition occurring in the water column. We acknowledge that photo-inhibition might be predicted to occur in some of the regions we visited. However, we have used the Galathea data to compare our calculation model for primary production where photo-inhibition is not taken into account, and another (Platt et al., 1980) where photo-inhibition is included. A strong linear relationship ($R^2 = 0.95$, $n = 82$) was revealed between the results obtained with the two models, where results using Platt's photo-inhibition model were approximately 27% lower than our model. We cannot explain why applying the photo-inhibition parameter in Platt's model should yield a more or less constant reduction in water column photosynthesis at high and low productive stations and under varying ambient light conditions. We, therefore, choose not to include photo-inhibition in our model.

2.7. Determination of export production

A pelagic food web model for determination of export production from primary production and temperature by Laws et al. (2000) was applied to the data set. Ideally, total primary production should be input to the model but, in the present study, particulate production has been used. The model is applied to the input variables of in-situ temperature and particulate production down through the euphotic zone and yields an estimate of export production at the station.

2.8. Determination of pCO_2 and sea–air CO_2 flux

Sea–air flux of CO_2 is calculated from the difference in partial pressure of CO_2 at the sea surface and in the atmosphere. The difference in pCO_2 gives the direction of the sea–air exchange and the potential uptake and the gas surface exchange coefficient is required to calculate actual flux rates of CO_2 (Liss and Merlivat, 1986, Wanninkhof, 1992, Nightingale et al., 2000). The exchange coefficients are usually parameterized as wind speed dependent and, in the present study, we use the parameterizations from Wanninkhof (1992). The average $\Delta pCO_2 = pCO_{2(sea)} - pCO_{2(air)}$, ocean temperature and salinity recorded during the period of time the ship was at the sampling station was used together with wind field data to calculate the sea–air CO_2 flux.

The partial pressure of CO_2 in the ocean is determined by bringing a volume of air into equilibrium with a continuous stream of seawater. For this, we used an equilibrator system where the CO_2 in the air sample coming from the equilibrator was measured using an IR CO_2 monitor (LICOR-6262). The CO_2 monitor, in turn, measured the air sample from the equilibrator system, a calibration gas and the atmospheric air. In this manner, we could use the same instrument for determining pCO_2 in the ocean and the atmosphere. The equilibrator was constructed following Dickson and Goyet (1994) and consists of a 10 l glass cylinder where water is pumped in at the top of the cylinder into the chamber where a series of small glass tubes increases the water–air contact surface in order to achieve equilibrium quickly. Air is sampled continuously from the equilibrator into the CO_2 monitor and the air flow from the CO_2 monitor is returned into the equilibrator in a circulating flow. The ocean–atmosphere difference in pCO_2 is determined as half-hour means during the cruise.

Data for the wind fields at the sampling station over the week prior to arrival at the station were obtained from the National Center for Environmental Prediction available at http://www.esrl.noaa.gov/psd/data/reanalysis/reanalysis.shtml. Based on the values for the wind field at 6 h intervals during this 1 week period and the measured average ΔpCO_2, ocean temperature and salinity at the station, a sea–air CO_2 flux was calculated for every 6 h and, subsequently, averaged for the 1-week period. The averaged sea–air CO_2 flux gives an estimate of the net amount of CO_2 that has been transported into/out of the ocean during the week prior to sampling. Thus, this approach provides a rate measurement that can be directly related to the rate measurement obtained for primary production, where it is assumed that that the primary production measurement obtained on a given sampling date is representative for the rate during the past week. (Note that primary production rates are estimated using weekly light averages.)

2.9. Estimation of temperature corrected pCO_2

Influence from the seasonal surface temperature changes on the pCO_2 was considered by removing the effect from the difference between the observed temperature (T_{obs}) and the local annual mean temperature (T_{mean}). For each station, the annual mean SST was determined by bilinear interpolation from the $1 \times 1°$ gridded World Ocean Atlas 2009 (Locarnini et al., 2010). From the temperature difference ($T_{mean} - T_{obs}$), the influence from seasonal temperature change on the pCO_2(obs) was calculated according to Takahashi et al. (2002): $pCO_2(T_{mean}) = pCO_2(obs.) \cdot \exp[0.0423(T_{mean} - T_{obs})]$, where $pCO_2(T_{mean})$ is the expected pCO_2 at annual mean temperature if only temperature effects account for the local pCO_2 changes. Subsequently, the influence on the sea–air CO_2 flux (F_{CO_2}) could be calculated from $F_{CO_2}(T_{corr}) = \gamma F_{CO_2}$, where the correction term is determined by $\gamma = (pCO_2(T_{mean}) - pCO_2(obs, air))/(pCO_2(obs, water) - pCO_2(obs, air))$. Correlations between calculated export production

and sea–air CO_2 fluxes were calculated for both the observed and the temperature corrected sea–air CO_2 flux.

2.10. Copepod abundance and potential production

As an indicator of the secondary production of the plankton ecosystem, we focused on the demography of calanoid and cyclopoid copepods. As copepod populations, in general, are found to be food limited, we assume that the number of juvenile stages in the population will be a reflection of the production. Therefore, we used as a proxy for production the ratio between the number of nauplii and the total abundance of copepods. Samples for determining the vertical distribution of metazooplankton ($> 50 \mu m$) were collected using a HYDRO-BIOS MultiNet Midi. The MultiNet consists of 5 nets with a closing option for 4 of the nets. The strata investigated were 0–50–100–200–300–400 m or 0–75–150–200–300–400 m. The MultiNet was lowered and hauled with speeds of 18 and 10 m min^{-1}, respectively. Samples were fixed in 4% formalin and stored at 5 °C prior to microscopic enumeration and calculation of the ratio of nauplii to total copepod abundance.

2.11. Statistical analyses

The data set describing fraction of phytoplankton $> 10 \mu m$ vs. temperature does not show homogeneity of variance before transformation. Therefore, a non-parametric Kruskal–Wallis test was used to compare the median of the fraction of total chlorophyll retained on a 10 μm filter in four temperature groups. The medians for each group were compared pair-wise using the Kruskal–Wallis test.

The multiple regressions were preceded by linear regressions and transformations to ensure that the data meet statistical assumptions of independence, homogeneity of variance, normality of error and linearity/additivity. The multiple linear regressions for $\log_{10}$(fraction of phytoplankton $> 10 \mu m + \delta_{cell size}$) vs. temperature, vs. $\log_{10}(DIN + \delta_{DIN})$, vs. $\log_{10}(PO_4 + d_{PO_4})$, vs. $\log_{10}(Si + \delta_{Si})$ and vs. depth demonstrate normality of error by the Lilliefors test. The individual regression coefficients in the multiple linear regressions are tested with a t-test. The offsets used in the transformation were $\delta_{DIN} = 0.04$, $d_{PO_4} = 0.06$ and $\delta_{Si} = 0.2 \mu mol/kg$ and $\delta_{cell size} = 0.001$. In the following, the transformed variables are referred to as $\log_{10}(DIN)$, $\log_{10}(PO_4)$, $\log_{10}(Si)$ and $\log_{10}$(fraction of phytoplankton $> 10 \mu m$) without explicitly writing the δ offsets.

An analysis of covariance (ANOCOVA) was performed on the transformed data set of $\log_{10}$(fraction of phytoplankton $> 10 \mu m$) vs. temperature. The data set is divided into two groups with high and low phosphate concentration and each group with index i is fitted to a model of the following type: $\log_{10}$(fraction of phytoplankton $> 10 \mu m)_i = \alpha_i + \beta_i \cdot$ temperature. Firstly, it is determined whether there is a significant relationship between community size and temperature for both groups. Secondly, it is tested whether the slopes of the regression lines for the two groups $\beta_{PO_4 > 0.29 \mu mol/kg}$ and $\beta_{PO_4 < 0.29 \mu mol/kg}$ are significantly different from one another using an F-statistic on the interaction term expressing the difference in slopes between the groups. Finally, if there is no difference between the slopes (i.e. the lines can be considered as being parallel), it is investigated whether there is homogeneity of the intercepts ($\alpha_{PO_4 \geq 0.29 \mu mol/kg}$ and $\alpha_{PO_4 < 0.29 \mu mol/kg}$). If the intercepts are not homogeneous, then we can deduce that there is a significant coupling between the phosphate concentration and the temperature. An equivalent analysis of covariance was done after dividing the data set into two groups with high and low DIN concentration. Here, the two

groups being tested were for DIN concentrations $<$ and $>$ 2.7 μmol/kg, respectively.

Mesozooplankton production vs. temperature was analyzed by linear regression. The data set of mesozooplankton production vs. cell size did, on the other hand, not show normality of error when doing linear regression. Therefore, a non-parametric Kruskal–Wallis test was used for comparing the median mezozooplankton production in the two approximately equally sized groups with the smallest and the largest cell size.

Linear regression analyses were performed on export and primary production vs. sea–air CO_2-flux in each of the geographical regions. The linear regressions were performed both for the raw and for the temperature-corrected sea–air CO_2-flux data.

The data set describing export production vs. integrated chlorophyll a did not show homogeneity of variance before transformation. Linear regressions and transformations were consequently performed to ensure that the data meet statistical assumptions and, subsequently, linear regressions were performed on $\log_{10}$(export production$+\delta_{EP}$) vs. $\log_{10}$(integrated chlorophyll $a+\delta_{Chl.\ a}$). The analysis was performed both for the northern North Atlantic and for the data set as a whole. The following data set was transformed and analyzed in the same way: $\log_{10}$(export production$+\delta_{EP}$) vs. $\log_{10}$(fraction of phytoplankton >10 μm$+\delta_{cell\ size}$). The offsets used in the transformation were $\delta_{EP}=0.008$ molC/m^2/day, $\delta_{cell\ size}=0.001$ and $\delta_{Chl.\ a}=10$ molC/m^2/day. In the following, the transformed variables are referred to without explicitly writing the δ offsets.

For the linear regressions, F-tests were applied to check how well the model fitted the data and normality of error was demonstrated by the Lilliefors test.

3. Results

3.1. Phytoplankton community size structure and temperature

A significant linear relationship was found between phytoplankton cell size and (a) temperature, (b) dissolved inorganic nitrogen (DIN) and (c) phosphate concentrations when the entire data set was examined (Fig. 1 and Table 2). The relationship between the fraction of the phytoplankton community >10 μm and temperature was, however, stronger ($p=0.00050$) than the relationship with the phosphate ($p=0.031$) and the dissolved

inorganic nitrogen ($p=0.034$). Fig. 1a, in which all data are plotted, illustrates that no phytoplankton communities were encountered in waters over 20 °C where cells larger than 10 μm comprised more than about 30% of the total chlorophyll concentration. The community size response to temperature is, however, marked over the entire temperature range encountered (i.e. from <0 to >30 °C). When the total data set is divided into four temperature groups and the median sizes of the communities found in the different groups are compared (Fig. 2), it can be seen that cells become progressively smaller over the entire temperature range studied. A comparison of the median sizes in the four temperature groups by a Kruskal–Wallis test indicates that the medians in all groups, except the two warmest, are significantly different.

That phytoplankton communities in warmer waters tend to be dominated by small cells is commonly reported. However, this is usually assumed to only be a function of nutrient availability as small size has been shown to be an advantage in nutrient limited conditions (see Kiørboe, 1993) and warm surface waters often indicate a stratified water body with limited nutrient delivery to surface waters. Therefore, we also tested the data set for possible relationships between inorganic nutrient availability and community cell size. No significant relationship between phytoplankton community size structure and silicate was found (Table 2).

Table 2

Statistics for multiple linear regression for $\log_{10}$(fraction of phytoplankton >10 μm) vs. temperature, vs. $\log_{10}$(DIN), vs. $\log_{10}$(PO$_4$), vs. $\log_{10}$(Si), and vs. depth. Adjusted $R^2=0.32$ for the overall fit with $N=262$ data points. DIN$=$NO$_3$$+NO_2$$+NH_4$. Individual regression coefficients and their standard errors are listed in the table. The individual regression coefficients are tested with a t-test, and t-value and p-value from the test are also listed in the table. Normality of error is demonstrated by the Kolmogorov–Smirnov test.

Variable	Regression coefficient	Standard error	t-value	p-value (t-test)
Temperature (°C)	-0.0161	0.0045	-3.52	0.00050
$\log_{10}$(DIN (μmol/kg))	0.131	0.061	2.13	0.034
$\log_{10}$(PO$_4$ (μmol/kg))	0.274	0.127	2.16	0.031
$\log_{10}$(Si (μmol/kg))	-0.120	0.075	-1.61	0.11
Depth (db)	-0.00164	0.00065	-2.54	0.012
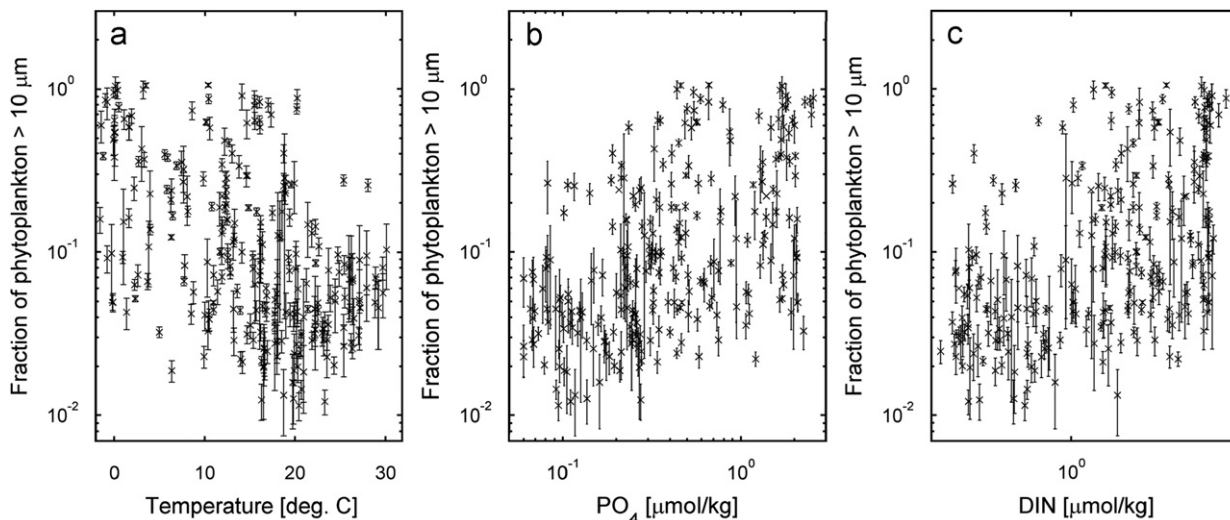
Fig. 1. Fraction of phytoplankton >10 μm vs. temperature (a), vs. DIN (b) and vs. PO$_4$ (c) using the global data set. The error bars show the propagated error on the fraction of phytoplankton >10 μm calculated from the standard deviations of the triplicate measurement of the chlorophyll a concentration, when the seawater was filtered on both the 10 μm and GF/F filters. DIN$=$NO$_3$$+NO_2$$+NH_4$. (The transformation offsets $\delta_{cell\ size}$, δ_{DIN} and δ_{PO4} are included in the data shown on the figures.)
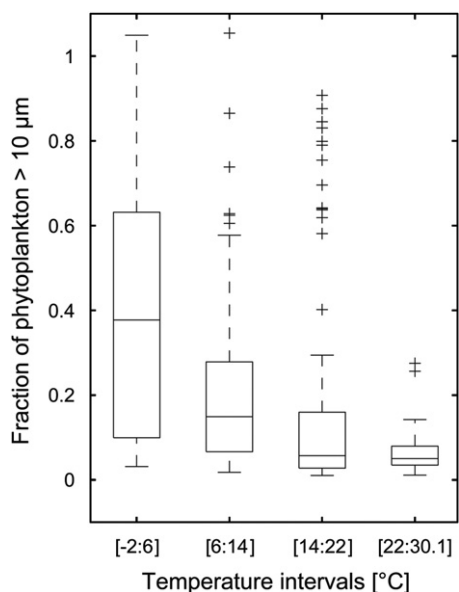
Fig. 2. Fraction of phytoplankton $> 10 \, \mu m$ vs. temperature using the global data set plotted in four temperature intervals. Data in each interval extend up to but do not include the highest temperature indicated. In each of the temperature intervals shown, the median of the data is indicated in the center of the box and the edges of the box are the 25th and 75th percentiles; the whiskers extend to the most extreme data points not considered outliers, and outliers are plotted individually. An analysis of the 4 intervals shows that the median of the phytoplankton size is significantly different (Kruskal–Wallice test $p < 0.005$) and decreasing with temperature. The only exception is the median of phytoplankton size in the intervals [14:22] and [22:30.1] °C, which is not significantly different ($p = 0.34$).

As noted above, we did find a weakly significant relationship between community size structure and both the total DIN and phosphate concentrations.

By dividing the data into groups with the highest and the lowest concentrations of phosphate and DIN, respectively, we were able to conduct further analyses that elucidated the potential interaction between nutrients and temperature on phytoplankton community size structure. To investigate whether there was a significant coupling between temperature and total DIN and/or phosphate, we split the data into two approximately equal sized groups representing the samples with the highest and the lowest concentrations of phosphate, (i.e. $\geq$ and $< 0.29 \, \mu mol/kg$) and performed an analysis of covariance. The relationship $\log_{10}(\text{fraction of phytoplankton} > 10 \, \mu m) = \beta_i \cdot \text{temperature} + \alpha_i$ between community size and temperature was significant for both the highest and the lowest concentrations of phosphate groups ($p < 0.001$). The slopes of the lines describing the relationship for the two subgroups were $\beta_{PO_4 \geq 0.29 \, \mu mol/kg} = -0.0199 \pm 0.0039$ ($N = 129$) and $\beta_{PO_4 < 0.29 \, \mu mol/kg} = -0.0194 \pm 0.0039$ ($N = 133$), and the lines could best be described as parallel (F-statistic $F = 0.0$; $p = 0.95$). Finally, we found that the data were better described by two parallel lines than by a single line (F-statistic $F = 27.2$; $p < 0.001$)), corresponding to the intercepts ($\alpha_{PO_4 \geq 0.29 \, \mu mol/kg} = -0.867 \pm 0.070$ and $\alpha_{PO_4 < 0.29 \, \mu mol/kg} = -0.543 \pm 0.070$). These intercepts were found to be significantly different.

Similarly, we split the data into two approximately equally sized groups representing the samples with the highest and the lowest concentrations of DIN (i.e. $\geq$ and $< 2.7 \, \mu mol/kg$) and performed the same analyses. The relationship $\log_{10}(\text{fraction of phytoplankton} > 10 \, \mu m) = \beta_i \cdot \text{temperature} + \alpha_i$ between community size and temperature was significant for both the highest and the lowest concentrations of DIN groups ($p < 0.005$). The slopes of the lines describing the relationship for the two subgroups were
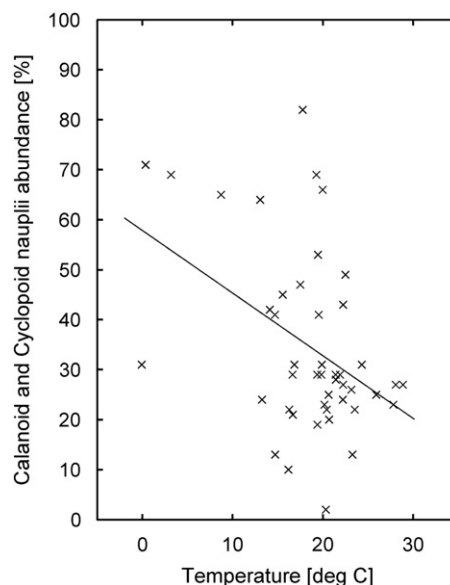
Fig. 3. The contribution of calanoid and cyclopoid copepod nauplii to the total abundance is used as a proxy for secondary production, here shown as a function of temperature using the global data set ($N = 45$).

$\beta_{(DIN \geq 2.7 \, \mu mol/kg)} = -0.0210 \pm 0.0042$ ($N = 132$) and $\beta_{(DIN < 2.7 \, \mu mol/kg)} = -0.0265 \pm 0.0042$ ($N = 130$) and the lines could best be described as parallel ($F = 0.43$; $p = 0.51$). Finally, the intercepts ($\alpha_{DIN \geq 2.7 \, \mu mol/kg} = -0.683 \pm 0.074$ and $\alpha_{DIN < 2.7 \, \mu mol/kg} = -0.583 \pm 0.074$) were found to be significantly different (F-statistic $F = 8.1$; $p < 0.005$).

The analyses imply that there is strong temperature effect on the cell size, and the fact that the data can be described by two parallel lines implies that there is an interaction between temperature and nutrients (both DIN and phosphate). Consequently, both nutrients and temperature emerge from this analysis as being important parameters for predicting the fraction of cells larger than $10 \, \mu m$. The analysis does not, however, allow us to separate and quantify the individual effects of temperature and nutrient availability, separately, on phytoplankton community size structure.

3.2. The relationship between mesozooplankton production and temperature

The fraction of the total abundances of calanoid and cyclopoid copepods made up of nauplii (used here as a proxy for mesozooplankton production) also decreased significantly ($p < 0.005$, $N = 45$) with increase in temperature (Fig. 3). There is no normality of error when doing linear regression of mesozooplankton production vs. cell size. Instead, the samples were grouped into two approximately equal sized groups with small and large cell sizes (i.e. the fraction of phytoplankton larger than $10 \, \mu m$ have values $<$ and > 0.45 individually in the two groups); we find that the mesozooplankton production is significantly lower in the group with the smallest phytoplankton cell size ($p = 0.036$ Kruskal–Wallis).

3.3. Export production and sea–air CO_2 flux

Fig. 4 illustrates the position of stations indicating, respectively, out-gassing or uptake of CO_2. Export production is plotted as a function of this out-gassing or uptake (i.e. sea–air CO_2 flux) in Fig. 5a (observed flux) and Fig. 5b (temperature corrected flux). There is a suggestion of increased export production with increase in ocean out-gassing of CO_2 (right hand side of both the figures). For most of the stations where out-gassing was observed, surface
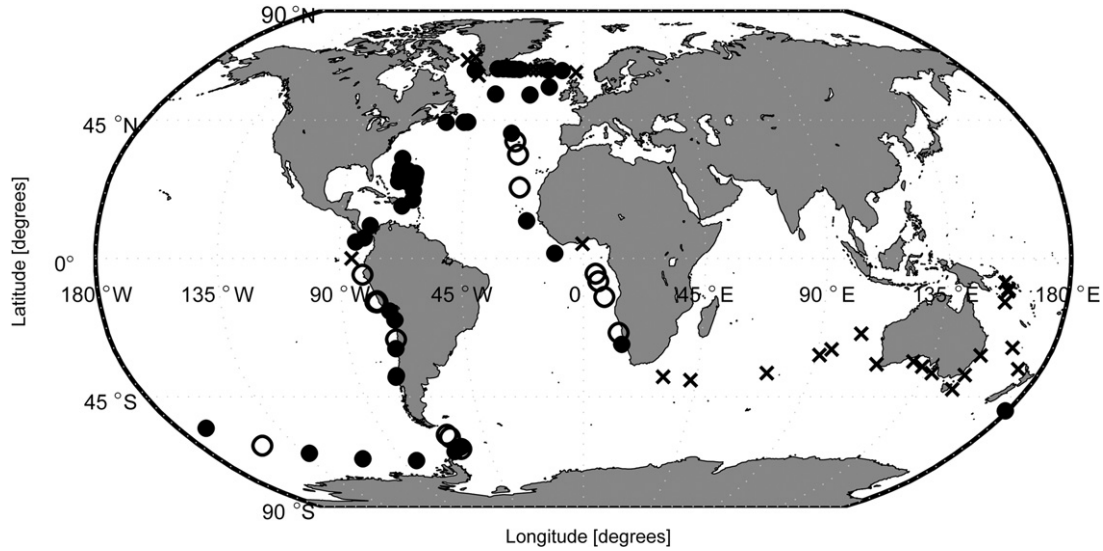
Fig. 4. Map of stations, filled and open circles symbolize CO_2 uptake and out-gassing. Crosses symbolize stations with no data for CO_2-flux.
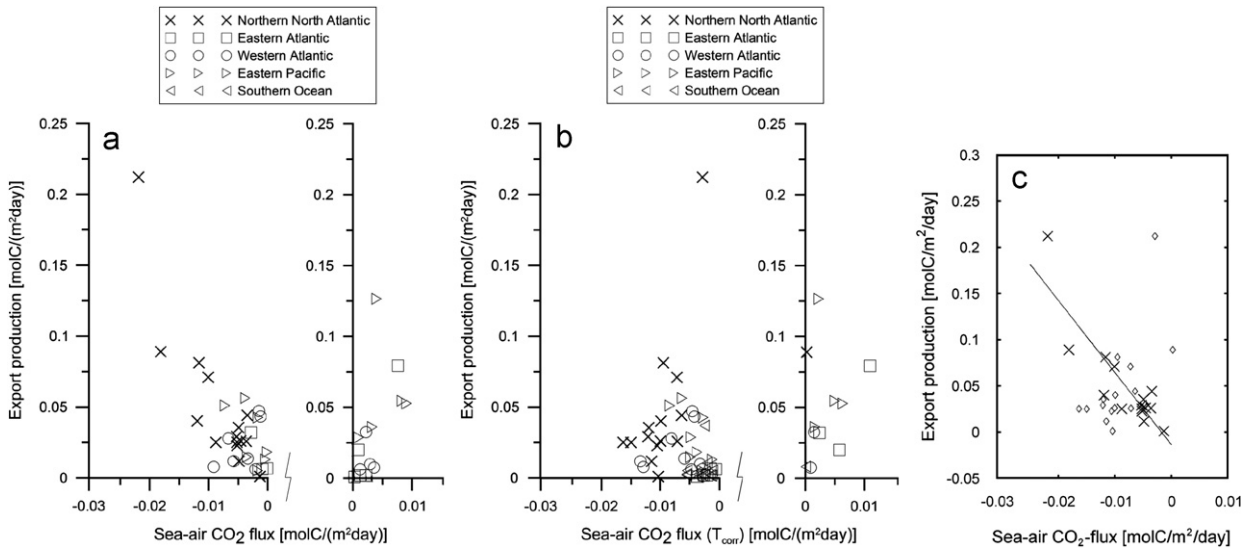

Fig. 5. Export production vs. sea–air CO_2-flux (a) and vs. temperature corrected sea–air CO_2-flux (b). Different symbols refer to different regions as described in the legend. Export production vs. sea–air CO_2-flux in Northern North Atlantic (c). Crosses show sea–air CO_2-flux without temperature correction, and diamonds show sea–air CO_2-flux with temperature correction. Line shows linear fit to data without temperature correction.

temperatures with respect to those of surrounding areas indicated the occurrence of recent upwelling (data not shown).
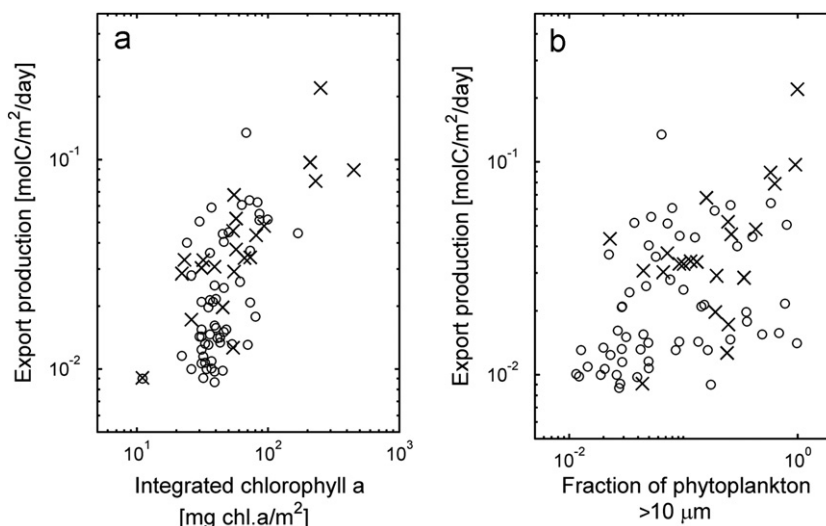
With respect to export production in regions where ocean uptake of CO_2 was recorded (left hand side of Fig. 5a and b), the seasonal data coverage is the best for the northern North Atlantic, where there are data from both early spring in 2007 and late summer in both 2006 and 2008. The apparent (but not significant) relationship between export production and ocean uptake of CO_2 seen in the non-temperature corrected data (Fig. 5a) is driven by these data from the northern North Atlantic. When all of the northern North Atlantic data are considered, the relationship between export (and primary, data not shown) production and observed CO_2 flux is highly significant ($p < 0.0001$; Table 3). On the other hand, without these spring data neither the northern North Atlantic nor other individual ocean basins demonstrated a significant relationship between ocean CO_2 uptake and export production. The flux calculated from the temperature corrected pCO_2 does not show a significant relationship between export production and

flux in the North Atlantic (Fig. 5c). Nevertheless, there is a suggestion of increasing export production with increase in influx also for these data.

Table 3
Linear regression for export production vs. sea–air CO_2-flux, with adjusted R^2, slope β and number of observations N. To check how well the linear regression model fits the data the F-test is applied and the p-value listed in the table.

Region	Adjusted R^2	β	N	p-value
Northern North Atlantic	0.77	−7.8	15	< 0.0001
Northern North Atlantic—no spring bloom	0.22	−2.0	10	0.17
Eastern Atlantic	0.43	5.7	8	0.076
Southern Ocean–no fit, not normality of error			11	
Eastern Pacific	0.11	2.2	12	0.30
Western Atlantic–no fit not normality of error			14	

Fig. 6. Export production vs. integrated water column chlorophyll *a* (a). Export production vs. fraction of phytoplankton $> 10 \, \mu m$ (b). Data for the northern North Atlantic is symbolized with crosses and the global data set is symbolized by the combination of all data points (circles and crosses together). (The transformation offsets $\delta_{cell \, size}$, δ_{EP} and $\delta_{Chl. \, a}$ are included in the data shown on the figures.)

3.4. Export production, water column chlorophyll and phytoplankton community size structure

There was a significant relationship ($p < 0.0001$, $N=79$, $R^2_{adjust}=0.43$) found in the data set between export production and integrated water column chlorophyll (Fig. 6a). The highest concentrations (up to 440 mg chlorophyll $a \, m^{-2}$) were observed in the northern North Atlantic data and it is data from this region that partially drive the signal found in the data set as a whole. For the northern North Atlantic alone, the relationship is significant both with ($p < 0.0001$, $N=22$, $R^2_{adjusted}=0.64$) and without ($p < 0.01$, $N=17$, $R^2_{adjusted}=0.35$) the inclusion of the spring bloom data.

Also phytoplankton community size structure is significantly correlated with export production (Fig. 6b) in the data set as a whole ($p < 0.0001$, $N=79$, $R^2_{adjusted}=0.23$). Again, much of the signal here is derived from the data from the northern North Atlantic ($p < 0.005$, $N=22$, $R^2_{adjusted}=0.29$), where seasonal coverage was the best. The linear regressions were performed on the transformed data as previously described.

4. Discussion

4.1. Phytoplankton community size structure and temperature

Both top-down (i.e. grazing) and bottom-up (i.e. nutrient availability) are important for establishing phytoplankton community size structure. With respect to the bottom-up determinants, it has traditionally been believed that it is nutrient availability that directly controls phytoplankton size (e.g. Kiørboe, 1993), The data set presented here suggests, however, that temperature also may have a direct effect on phytoplankton size and, thereby, influence phytoplankton community size structure.

The analysis here reveals a strongly significant relationship between size structure of the phytoplankton community in open ocean communities and water temperature (Figs. 1 and 2; Table 2) where the fraction of total chlorophyll retained on a $> 10 \, \mu m$ filter decreases as temperature increases. In waters where the temperature was over 20 °C, no stations where large cells contributed with more than approximately 30% of the total chlorophyll were encountered.

Laws et al. (2000) argued that at temperatures over 25 °C, the magnitude of export production was insensitive to the magnitude of primary production and that this temperature influence on export production is qualitatively easy to understand as rates of microbial degradation are the greatest under warm conditions. Thus, when temperatures are high, a relatively small proportion of the organic material generated in the surface waters will sink.

In addition to bacterial degradation of organic material being the greatest in warm waters, the data presented here confirm the assumption in Laws et al.'s model that small cells dominate in warm waters. Initially, when we observed this relationship between cell size and water temperature, we assumed that the underlying cause was nutrient availability as warmer waters may be expected to be more stratified and, therefore, more likely to be nutrient depleted in the euphotic zone. We were not able to demonstrate a significant relationship between silicate availability and cell size. We did find a statistically significant relationship between phytoplankton community size structure and both DIN (nitrate, nitrite and ammonium) and phosphate availabilities. However, in neither case was the relationship as strong as the relationship between community size structure and temperature.

We divided the data set into two groups and compared the relationship between community cell size and temperature for the half of the data with the highest and the lowest phosphate and DIN concentrations, respectively. In both subgroups, there was a persistent strong relation between temperature and community cell size. We found the slopes of the resulting regression lines not to be significantly different, but we did find that the intercepts for the linear fits for the two groups were significantly different, indicating that there is an interaction between temperature and nutrients. Consequently, we conclude that both temperature and nutrients may be controlling factors in community size structure.

Although several authors (e.g. Agawin et al., 2000; Morán et al. (2010)) have noted an increased abundance of picoplankton in warmer waters, a relationship between temperature and phytoplankton community size structure has, as far as we know, not previously been demonstrated on a data set for natural phytoplankton communities comprising samples from such a wide geographic area. A temperature effect on size has, however, been noted earlier within individual species of phytoplankton: the cells of individual diatom species, for example, when exposed to differing growth temperatures, generally follow the rule of

decreasing cell size with increasing temperatures in the same manner as other ectotherms (Atkinson, 1994, 1995). We note, though, that no satisfactory explanation for this observation has yet been offered (Montagnes and Franklin, 2001).

Following the logic of Laws et al. (2000), we suggest that one possible explanation for the observed temperature response in phytoplankton community size structure could be the increase in competition with heterotrophs for access to nutrients with increase in temperature. Surface to volume ratio has long been argued to be important for nutrient uptake (e.g. Kiørboe, 1993), where small cells are believed to have a competitive advantage under limiting nutrient conditions. As heterotrophic activity increases with increase in temperature, one could envision that increased competition between phytoplankton and heterotrophs for nutrients might lead to phytoplankton communities dominated by small cells. That Morán et al. (2010) recorded a marked increase in abundance of bacterioplankton concomitant with a decrease in nanoplankton and an increase in picoplankton as temperatures increased and salinity decreased in their study in Arctic waters confirms that bacteria populations under natural conditions respond to even small temperature changes. Also other heterotrophs than bacteria potentially compete with phototrophic phytoplankton for nutrients. Rose and Caron (2007) reviewed the relationship between the growth rate of herbivorous protists and the temperature and found the growth rates of the heterotrophs to be more sensitive to temperature than those of photoautotrophs. They also found that maximum growth rates of herbivorous protists equaled or exceeded those of photoautotrophs at temperatures over 15 °C. Thus, it appears that increasing temperatures are likely to increase nutrient competition between photoautotrophic phytoplankton and heterotrophs and it is possible that the decrease in size noted for phytoplankton with increasing temperature may be a consequence of this increased competition.

Regardless of the cause, a decrease in phytoplankton size with water temperature will have consequences on the sinking rate and the magnitude of export production. Surface ocean temperatures have been documented to be increasing (Domingues, et al., 2008; Levitus et al., 2009) in response to changes in the climate system. Our data suggest that the temperature increases recorded and those expected in the future potentially impact the size structure of the phytoplankton community and, thus, the magnitude of export production.

In addition to sinking rate, there are also differences between large and small phytoplankton cells with respect to their production of dissolved organic material. The importance of cell size for export production has previously been included in organic carbon export models such that small cell sizes imply a relatively higher production of dissolved organic carbon compared to particulate organic carbon (i.e. Laws et al., 2000). The global export of dissolved organic carbon has been estimated to be about 0.17 Pg C yr^{-1} (Hansell and Carlson, 1998), corresponding to about 10–20% of the global export production of about 10 Pg C yr^{-1} (Dunne et al., 2007). Therefore, a relative increase in small phytoplankton cell sizes in a warmer ocean could affect the global carbon export significantly through an increased dissolved organic carbon export and, thereby, a shallower remineralization of organic carbon.

Correspondingly, a temperature influence on phytoplankton size has implications for the particulate organic carbon export during colder climatic regimes where colder surface water would increase phytoplankton cell sizes and, potentially, increase deep-sea organic matter sedimentation, in accordance with analysis of glacial sediments (Kohfeld et al., 2005). However, the explicit relationship between phytoplankton cell size and remineralization depth of the sinking particulate organic carbon flux is complex and involves other factors such as the formation of aggregates and the particles associated content of mineral particles (De La Rocha and Passow,

2007). Thus, the potential consequences of a change in phytoplankton size for the remineralization depth of particulate organic carbon need to be further examined.

4.2. Temperature and mesozooplankton production

Not only biogeochemical fluxes but also food web structure can be expected to be impacted when small cells become more dominant in phytoplankton communities (e.g. Cushing, 1989; Kiørboe, 1993). To examine whether there was a global pattern in the structure of plankton food webs in relation to temperature or phytoplankton cell size, we here used a proxy for mesozooplankton production (the number of calanoid and cyclopoid nauplii as a percentage of the total number of calanoid and cyclopoid copepods recorded at a station/depth strata). The data set is smaller than the data set pertaining to phytoplankton, which impacts the statistical significance of the analyses.

Nevertheless, a strongly significant relationship was found in the data set between mesozooplankton production and temperature. Mesozooplankton production also was found to be significantly lower when the phytoplankton community was dominated by small cells than when it was dominated by large. It has often been demonstrated that phytoplankton cell size is an important factor in determining copepod production as the ability of these organisms to retain small particles in the feeding apparatus is limited (Bergreen et al., 1988, Kiørboe and Nielsen, 1994). Thus, the copepod community in warmer waters, where small phytoplankton become dominant, can be predicted to be less productive than copepod communities in colder waters because the copepods have to rely on microzooplankton to make the primary production available to them (Satapoomin et al., 2004). Consequently, a relatively larger fraction of the phytoplankton in warmer waters is recycled in the surface layer through the microbial food web rather than being sequestered to the deep water as large fast sinking fecal pellets (Møller et al., 2011).

4.3. Export production and phytoplankton community size structure

The significant correlation between phytoplankton community size structure and export production noted here is in accordance with the general understanding of how export production is regulated by ecosystem function in the euphotic zone, although few observations have confirmed such a connection directly. Phytoplankton size classes are, for example, included in the export production model of Laws et al. (2000) where large and small phytoplankton compartments constitute the ecosystem and the large compartment has relatively few trophic levels between primary production and export in contrast to the small phytoplankton group where several trophic levels leads to a reduction in the *f*-ratio. Their model is used to calculate export production in our study and, although the model only uses primary production and temperature as state variables, our results showing a correlation to phytoplankton size is seen to be in very good accordance with their assumptions.

In addition to phytoplankton cells and aggregates, however, many other factors are assumed to affect export of organic material, i.e. ballasting minerals as silica, calcium carbonate and lithogenic material (see review in Boyd and Trull, 2007) and, therefore, a simple relationship between size classes and EP is not expected. Recent analysis of direct observations by underwater video profiling of particle sizes in the mesopelagic zone (400 m) showed a significant relationship to size structure in the surface phytoplankton community, where communities dominated by picophytoplankton had a smaller export than communities dominated by microphytoplankton (Guidi et al., 2009). Our results are in good accordance with these findings. That a relationship between the size structure of the phytoplankton community and export production is found here

emphasizes the potential importance of biological diversity and activity in controlling the capacity of the ocean to serve as a natural carbon sink.

4.4. Phytoplankton activity and sea–air CO_2 flux

There is also a suggestion in the data presented here that biological activity and diversity may be important factors in determining the magnitude of sea–air CO_2 flux. With relatively few data points in each ocean basin, temperature correction of surface pCO_2 can only be achieved by drawing on published databases describing annual seasonal temperature and pCO_2 patterns. These databases present data averaged over relatively large ocean regions and, in using them to temperature correct the data collected here, we potentially introduce significant error. We, therefore, present export production as a function of both the actual flux we measured during the cruises and as a function of temperature corrected flux. In the non-corrected data, a very significant ($p < 0.0001$) relationship between export production and CO_2 flux was noted for the northern North Atlantic. The relationship is driven by the spring bloom measurements made here. However, even when the two highest points are removed from the statistical analysis, the relationship is still very significant ($p < 0.005$). In no other ocean basin was such a relationship noted. This may, however, be due to the limited seasonal distribution of data from the other ocean basins.

Temperature correction of the data changed the relative position of two data points from stations located in the large temperature gradient area between water masses from the North Atlantic and Labrador currents (Fig. 5b and c). The temperature correction, itself, could therefore introduce large errors into the data analysis, which are difficult to assess, in particular in this region.

In the temperature corrected data, the significant relationship between export production and sea–air CO_2 flux is no longer present and seasonal temperature changes should, therefore, be considered as a possible explanation for the observed relationship.

Nevertheless, the very strong relationship between export production (and thereby size structure in the phytoplankton community) and our sea–air CO_2 flux in the northern North Atlantic suggest that the potential role of phytoplankton activity and diversity in driving this flux at different times of the year should be investigated further especially given that two recent studies (Takahashi et al. (2009); Körtzinger et al. (2008)) suggest that some anomalies in the pCO_2 data they present for the North Atlantic might possibly be explained by biological activity.

The data presented here also indicate a positive relationship between out-gassing of CO_2 from the surface ocean and the phytoplankton photosynthesis/export production in some ocean basins. This relationship was expected, as out-gassing is often associated with upwelling of nutrient-rich bottom water to the surface and the introduction of nutrients to the surface layer can stimulate phytoplankton activity.

5. Conclusions

Given the importance of the ocean as a natural carbon sink and, not least of which the suggestion that this sink may be weakening (Le Quéré et al., 2009), there is concerted research effort being devoted to quantifying the factors influencing the function of this sink and how these factors may be altered by changing ocean conditions. This study suggests that temperature may have a direct effect on phytoplankton size and, thus, community size structure. The data set demonstrates that small cells become increasingly dominant in the community with increasing temperatures over a temperature range from < 0 to $> 30\,°C$. Inorganic nutrient availability and temperature in surface

waters of the ocean co-vary and it is traditionally assumed that phytoplankton size is directly controlled by nutrient availability. The analyses presented here, however, indicate that there may also be a direct effect of temperature on phytoplankton size. This suggests an increase in dominance of small cells in ocean phytoplankton communities in response to global ocean warming which, in turn, will impact plankton food web structure as well as impact the ocean's capacity to function as a natural carbon sink.

References

Agawin, N.S.R., Duarte, C.M., Agustı́, S., 2000. Nutrient and temperature control of the contribution of picoplankton to phytoplankton biomass and production. Limnology and Oceanography 45 (3), 591–600.

Atkinson, D., 1994. Temperature and organism size – a biological law for ectotherms? Advances in Ecological Research 25, 1–58.

Atkinson, D., 1995. Effects of temperature on the size of aquatic ectotherms: exceptions to the general rule. Journal of Thermal Biology. doi:10.1016/0306–4565(94)00028-H.

Bennington, V., McKinley, G.A., Dutkiewicz, S., Ullman, D., 2009. What does chlorophyll variability tell us about export and air–sea CO_2 flux variability in the North Atlantic? Global Biogeochemical Cycles 23, GB3002. doi:10.1029/2008GB003241.

Berggreen, U., Hansen, B., Kiørboe, T., 1988. Food size spectra, ingestion and growth of the copepod Acartia tonsa during development: implications for determination of copepod production. Marine Biology 99, 341–352.

Boyd, P.W., Trull, T.W., 2007. Understanding the export of biogenic particles in oceanic waters: is there consensus? Progress in Oceanography 72, 276–312.

Cushing, D.H., 1989. A difference in structure between ecosystems in strongly stratified waters and those that are only weakly stratified. Journal of Plankton Research 11, 1–13.

De La Rocha, C.L., Passow, U., 2007. Factors influencing the sinking of POC and the efficiency of the biological pump. Deep Sea Research II 54, 639–658.

Dickson, A.G., Goyet C. (Eds.), 1994. Handbook of Methods for the Analysis of the Various Parameters of the Carbon Dioxide System in Sea Water, version 2, ORNL/CDIAC-74.

Domingues, C.M., Church, J.A., White, N.J., Gleckler, P.J., Wijffels, S.E., Barker, P.M., Dunn, J.R., 2008. Improved estimates of upper-ocean warming and multi-decadal sea-level rise. Nature 453, 1090–1094.

Dunne, J.P., Sarmiento, J.L., Gnadadesikan, A., 2007. A synthesis of global particle export from the surface ocean and cycling through the ocean interior and on the seafloor. Global Biogeochemical Cycles 21, GB4006. doi:10.1029/2006GB002907.

Finkel, Z.V., Sebbo, J., Feist-Burkhardt, S., Irwin, A.J., Katz, M.E., Schofield, O.M.E., Young, J.R., Falkowski, P.G., 2007. A universal driver of macroevolutionary change in the size of marine phytoplankton over the. Cenozoic Proceedings of the National Academy of Science 104 (51), 20416–20420. doi:10.1073/pnas.0709381104 published ahead of print.

Grasshoff, K., Erhardt, M., Kremling, K., 1983. Methods of Seawater Analysis, 2. Revision. Verlag Chemie, Weinheim.

Guidi, L., Stemmann, L., Jackson, G.A., Ibanez, F., Claustre, H., Legendre, L., Picheral, M., Gorsky, G.l, 2009. Effects of phytoplankton community on production, size and export of large aggregates: a world-ocean analysis. Limnology and Oceanography 54 (6), 1951–1963.

Hansell, D.A., Carlson, C.A., 1998. Net community production of dissolved organic carbon. Global Biogeochemical Cycles 12, 443–453.

Kiørboe, T., 1993. Turbulence, phytoplankton cell size, and the structure of pelagic food webs. Advances in Marine Biology 29, 1–72.

Kiørboe, T., Nielsen, T.G., 1994. Regulation of zooplankton biomass and production in a temperate, coastal ecosystem. I. Copepods. Limnology and Oceanography 39, 493–507.

Kohfeld, K.E., Quéré, C.L., Harrison, S.P., Anderson, R.F., 2005. Role of the biology in glacial-interglacial CO_2 cycles. Science 308, 74–78.

Körtzinger, A., Send, U., Lampitt, R.S., Hartman, S., Wallace, D.W.R., Karstensen, J., Villagarcia, M.G., Llinaš, O., DeGrandpre, M.D., 2008. The seasonal pCO_2 cycle at 49_N/16.5_W in the northeastern Atlantic Ocean and what it tells us about biological productivity. Journal of Geophysical Reasearch 113, C04020. doi:10.1029/2007JC004347.

Khatiwala, S., Primeau, F., Hall, T., 2009. Reconstruction of anthropogenic CO_2 concentrations in the ocean. Nature 462, 346–349.

Laws, E.A., Falkowski, P.G., Smith Jr., W.O., Ducklow, H., McCarthy, J.J., 2000. Temperature effects on export production in the open ocean. Global Biogeochemical Cycles 14, 1231–1246.

Levitus, S., Antonov, J.I., Boyer, T.P., Locarnini, R.A., Garcia, H.E., Mishonov, A.V., 2009. Global ocean heat content 1955–2008 in light of recently revealed instrumentation problems. Geophysical Research Letters 36, L07608.

Le Quéré, C., Raupach, M.R., Canadell, J.G., Marland, G., Bopp, L., Ciais, P., Conway, T.J., Doney, S.C., Feely, R.A., Foster, P., Friedlingstein, P., Gurney, K., Houghton, R.A., House, J.I., Huntingford, C., Levy, P.E., Lomas, M.R., Majkut, J., Metzl, N., Ometto, J.P., Peters, G.P., Prentice, I.C., Randerson, J.T., Running, S.W., Sarmiento, J.L., Schuster, U., Sitch, S., Takahashi, T., Viovy, N., van der Werf, G.R., Woodward, F.I., 2009. Trends in the sources and sinks of carbon dioxide. Nature Geoscience 2, 831–836.

Li, W.K.W., McLaughlin, F.A., Lovejoy, C., Carmack, E.C., 2009. Smallest algae thrive as the Arctic ocean freshens. Science 326, 539.

Liss, P.S., Merlivat, L., 1986. Air-sea gas exchange rates: introduction and synthesis. In: Buat-Menard, P. (Ed.), The Role of Air–Sea Exchange in Geochemical Cycling. Springer, New York, pp. 113–127.

Locarnini, R.A., Mishonov, A.V., Antonov, J.I., Boyer, T.P., Garcia, H.E., Baranova, O.K., Zweng, M.M., Johnson, D.R., 2010. World Ocean Atlas 2009. In: Levitus, Temperature.S (Ed.), NOAA Atlas NESDIS 68, vol. 1. U.S. Government Printing Office, Washington, D.C, pp. 184.

Montagnes, D.J.S., Franklin, D.J., 2001. Effect of temperature on diatom volume, growth rate, and carbon and nitrogen content: reconsidering some paradigms. Limnology and Oceanography 46 (8), 2008–2018.

Morán, X.A., López-Urrutia, Á., Calvo-Díaz, Li, W.K.W., 2010. Increasing importance of small phytoplankton in a warmer ocean. Global Change Biology 16, 1137–1144. doi:10.1111/j.1365-2486.2009.01960.x.

Møller, E.F., Andersen, C.M., Jaspers, C., Satapoomin, Jonasdottir S, S Nielsen, T.G., 2011. Production and vertical export of copepod fecal pellets in the southern Indian Ocean. Marine Biology 158 (3), 677–688.

Nightingale, P.D., Malin, G., Law, C.S., Watson, A.J., Liss, P.S., Liddicoat, M.I., Boutin, J., Upstill-Goddard, R.C., 2000. In situ evaluation of air–sea gas exchange parameterizations using novel conservative and volatile tracers. Global Biogeochemical Cycles. 14, 373–387.

Platt, T., Gallegos, C.L., Harrison, W.G., 1980. Photoinhibition of photosynthesis in natural assemblages of marine phytoplankton. Journal of Marine Research 38, 687–701.

Rose, J.M., Caron, D.A., 2007. Does low temperature constrain the growth rates of heterotrophic protists? Evidence and implications for algal blooms in cold waters. Limnology and Oceanography 52 (2), 8886–8895.

Sabine, C.L., Feely, R.A., Gruber, N., Key, R.M., Lee, K., Bullister, J.L., Wanninkhof, R., Wong, C.S., Wallace, D.W.R., Tilbrook, B., Millero, F.J., Peng, T.-H., Kozyr, A., Ono, T., Rios, A.F., 2004. The oceanic sink for anthropogenic CO_2. Science 305, 367.

Sarmiento, J.L., Hughes, T.M.C., Stouffer, R.J., Manabe, S., 1998. Simulated response of the ocean carbon cycle to anthropogenic climate warming. Nature 393, 245–249.

Satapoomin, S., Nielsen, T.G., Hansen, P.J., 2004. Andaman Sea copepods: spatio-temporal variations in biomass and production, and role in the pelagic food web. Marine Ecology Progress Series 274, 99–122.

Steemann Nielsen, E., 1952. The use of radio-active carbon (C14) for measuring organic production in the sea. Journal du conseil/Conseil *international* pour l' *exploration* de la *mer* 18, 117–140.

Takahashi, T., Sutherland, S.C., Sweeney, C., Poisson, A., Metzl, N., Tillbrook, B., Bates, N., Wanninkhof, R., Feely, R.A., Sabine, C., Olafsson, J., Nojiri, Y., 2002. Global sea–air CO_2 flux based on climatological surface ocean pCO_2, and seasonal biological and temperature effects. Deep-Sea Research II 49, 1601–1622.

Takahashi, T., Sutherland, S.C., Wanninkhof, R., Sweeney, C., Feely, R.A., Chipman, D.W., Hales, B., Friederich, G., Chavez, F., Sabine, C., Watson, A., Bakker, D.C.E., Schuster, U., Metzl, N., Yoshikawa-Inoue, H., Ishii, M., Midorikawa, T., Nojiri, Y., Körtzinger, A., Steinhoff, T., Hoppema, M., Olafsson, J., Arnarson, T.S., Tilbrook, B., Johannessen, T., Olsen, A., Bellerby, R., Wong, C.S., Delille, B., Bates, N.R., de Baar, H.J.W., 2009. Climatological mean and decadal change in surface ocean pCO_2, and net sea–air CO_2 flux over the global oceans. Deep-Sea Research II 56, 554–5772009.

Wanninkhof, R., 1992. Relationship between wind speed and gas exchange over the ocean. Journal of Geophysical Research 97, 7373–7381.